Electronic Supplementary Material (ESI) for Journal of Materials Chemistry A.

Supplementary Information

Regulating lithium deposition behavior by electrokinetic effects in high-zeta-potential h-BN/zinc-lithium alloy for high-performance lithium metal anodes

Shipeng Liu, [b] Jingteng Zhao, [a] Fang Li, [a] Yingjie Zhao [b] and Guoxing Li *[a]

[a] *Science Center for Material Creation and Energy Conversion, Institute of Frontier and Interdisciplinary Science, Shandong University, Qingdao, 266237, China.*

[b] *College of Polymer Science and Engineering, Qingdao University of Science and Technology, Qingdao 266042, China.*

*Corresponding author:

E-mail: gxli@sdu.edu.cn

1. Supplementary figures

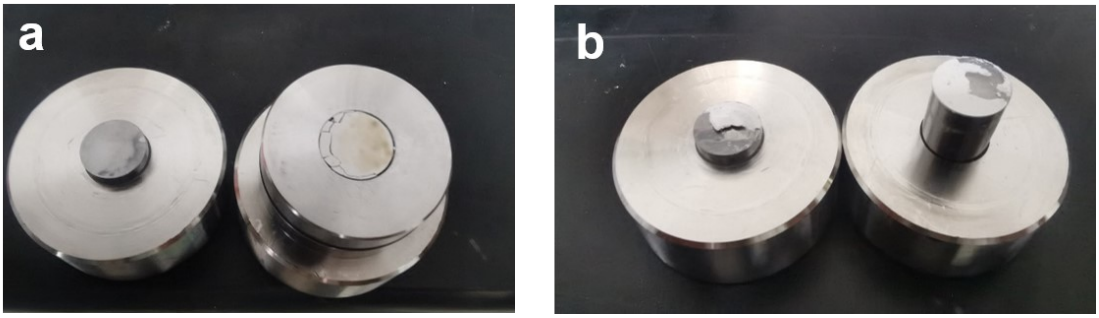

Fig. S1 Optical images of the prepared (a) pure ZnO film and (b) pure h-BN film.

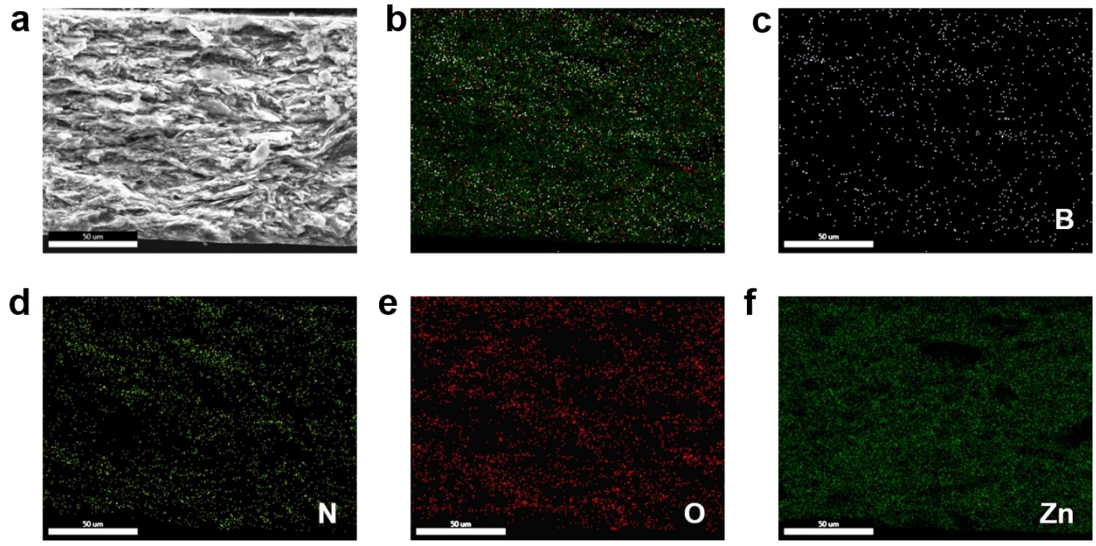

Fig. S2 SEM elemental mapping results of the ZB-film. (a) Cross-section SEM image of the ZB-film. (b) The homogenous distribution of B, N, O, Zn elements in the ZB film. EDS elemental mapping of (c) B, (d) N, (e) O, and (f) Zn.

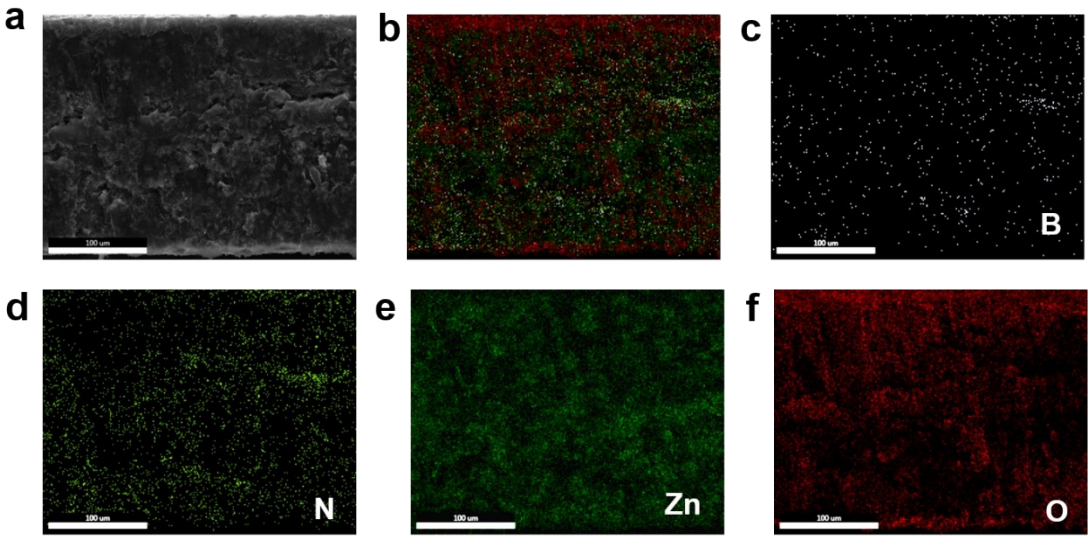

Fig. S3 SEM elemental mapping results of the Li-ZB. (a) Cross-section SEM image of the Li-ZB. (b) The homogenous distribution of B, N, O, Zn elements in the Li-ZB film. EDS elemental mapping of (c) B, (d) N, (e) Zn, and (f) O.

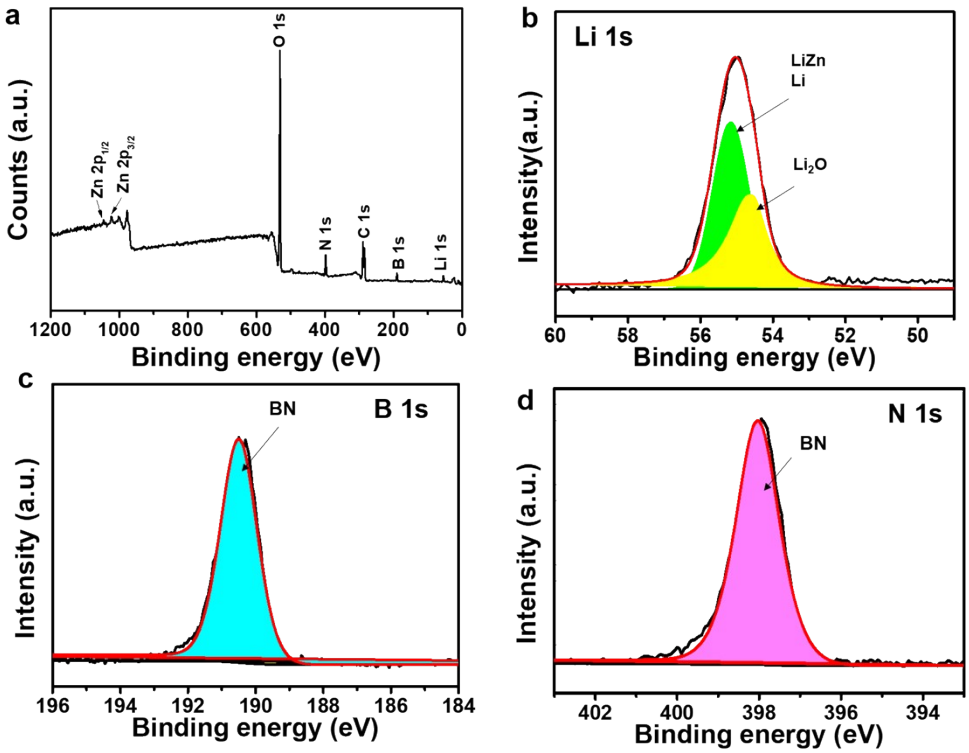

Fig. S4 XPS spectra of Li-ZB. (a) The XPS spectrum shows the presence of Li, Zn, B, N and O elements in the Li-ZB. High-resolution XPS spectra of (b) Li 1s, (c) B 1s, and (d) N 1s.

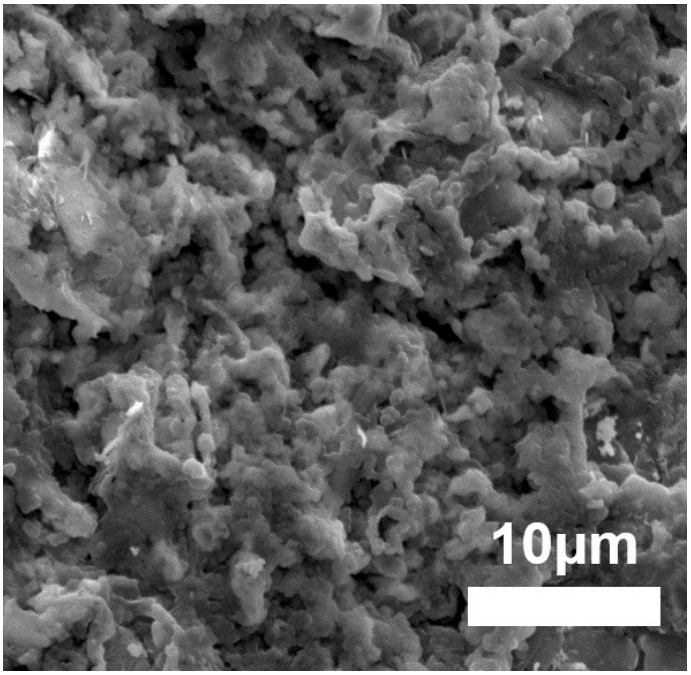

Fig. S5 The conformal porous structure formed on the surface of Li-ZB electrode after the initial Li stripping process.

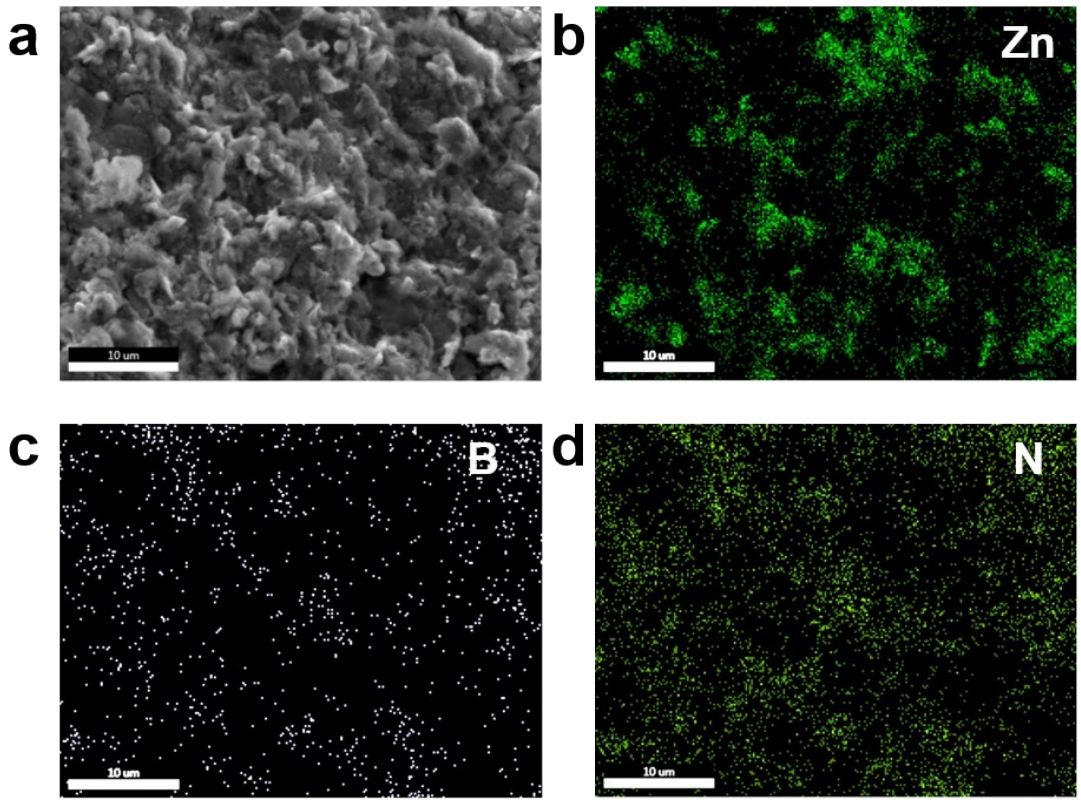

Fig. S6 SEM elemental mapping results of the conformal porous structure. (a) Top-view SEM image. EDS elemental mapping of (b) Zn, (c) B, and (d) N.

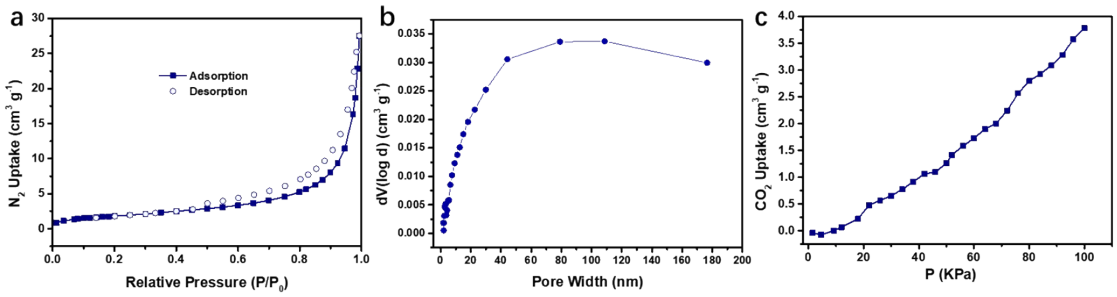

Fig. S7 BET surface area analysis. (a) N_2 adsorption-desorption isotherms of ZB film. (b) Pore size distribution from the nonlocal density functional theory of ZB film. (c) CO_2 adsorption isotherms of Li-ZB after stripping Li. The result shows the ZB film also contains many micro/meso pores. We performed the CO_2 adsorption experiments to study the porosity of Li-ZB after stripping certain amount of Li, and found that the CO_2 uptake of Li-ZB is 3.78 cm^3 g^{-1} at 298 K, indicating that it contains the micro/meso pores besides the observed micrometer-sized pores.

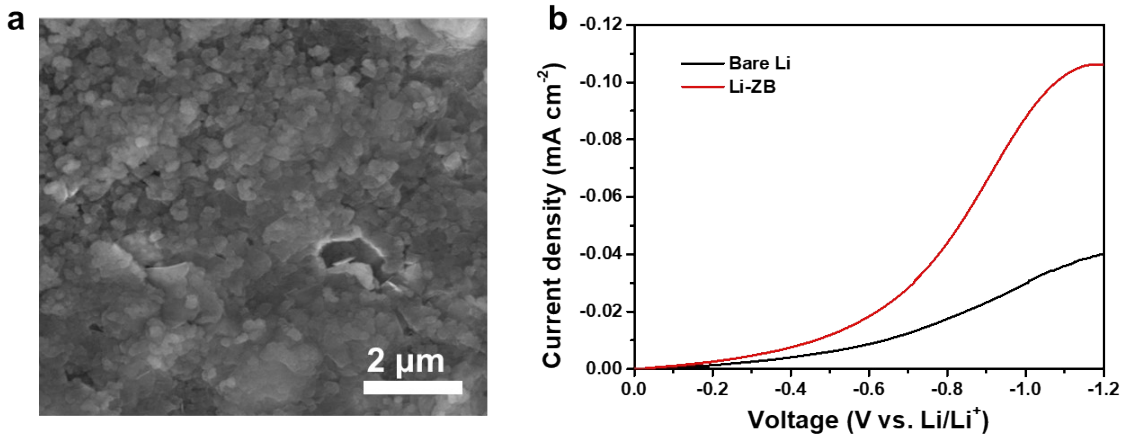

Fig. S8 (a) The SEM image of original Li-ZB, showing the micro/meso pores on its surface. (b) LSV curves of Li-ZB and bare Li electrodes.

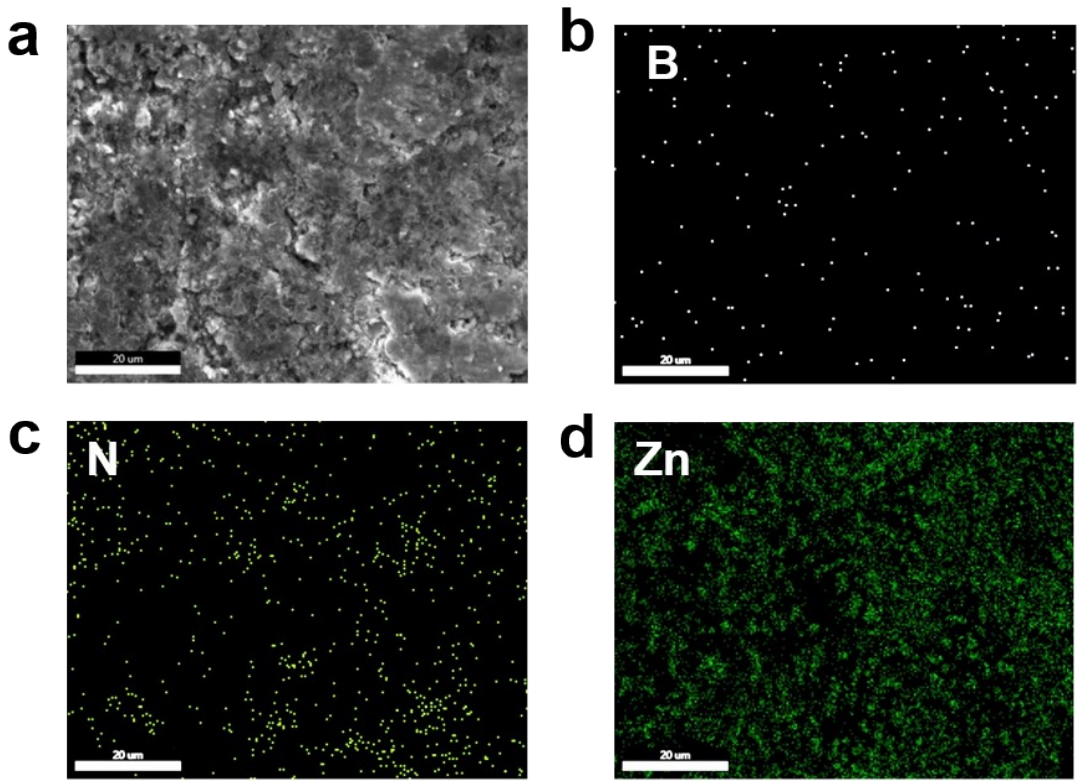

Fig. S9 SEM elemental mapping results of the cycled Li-ZB electrode. (a) Top-view SEM image. EDS elemental mapping of (b) B, (c) N, and (d) Zn.

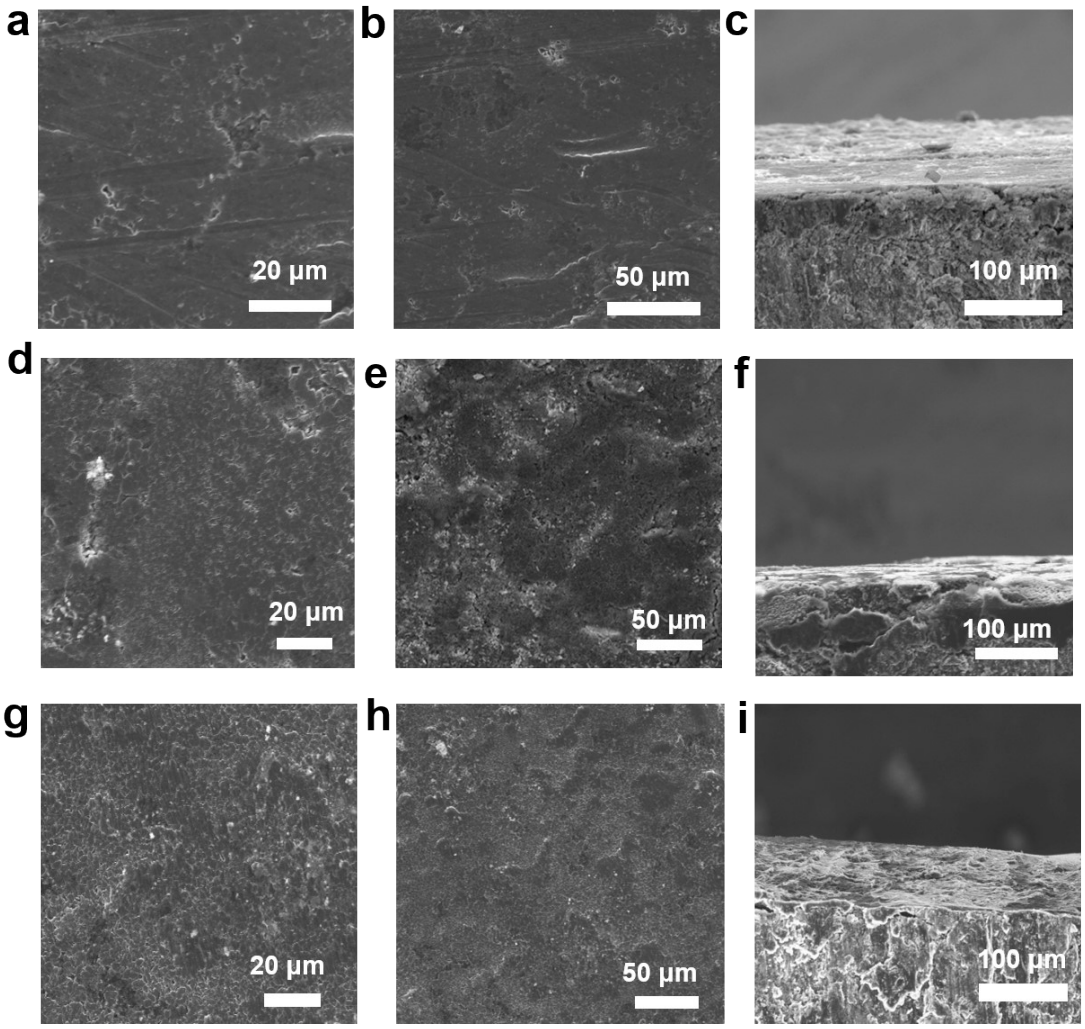

Fig. S10 Morphologies of of Li-ZB electrodes after cycling under high deposition capacities and current densities. (a, b) Top-view and (c) cross-section SEM images of Li-ZB after cycling at a current density of 4 mA cm^{-2} and a deposition capacity of 4 mA h cm^{-2}. (d, e) Top-view and (f) cross-section SEM images of Li-ZB after cycling at a current density of 6 mA cm^{-2} and a deposition capacity of 6 mA h cm^{-2}. (g, h) Top-view and (i) cross-section SEM images of Li-ZB after cycling at a current density of 8 mA cm^{-2} and a deposition capacity of 8 mA h cm^{-2}.

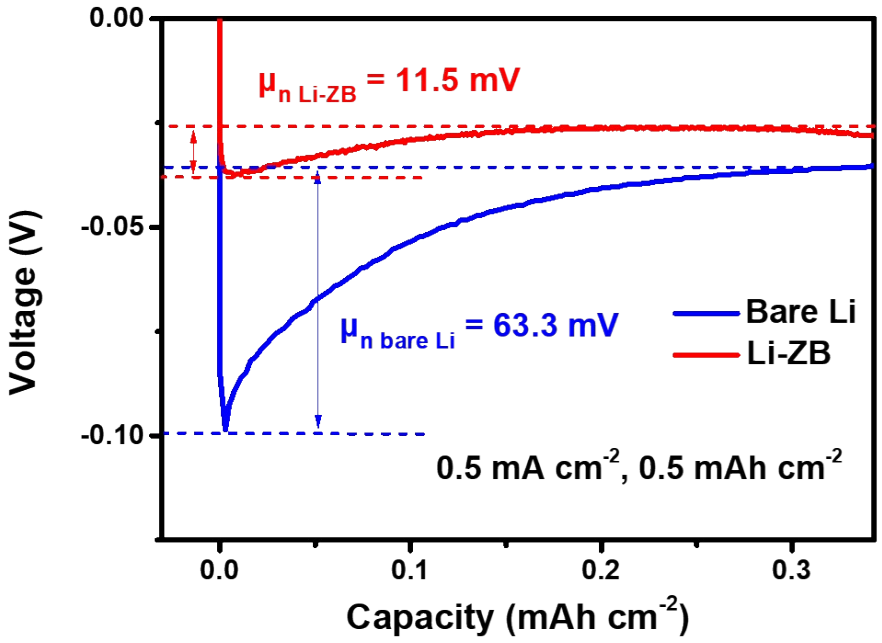

Fig. S11 Voltage-capacity curves of the Li-ZB and bare Li electrodes during Li plating at a current density of 0.5 mA cm^{-2} and a deposition capacity of 0.5 mA h cm^{-2}.

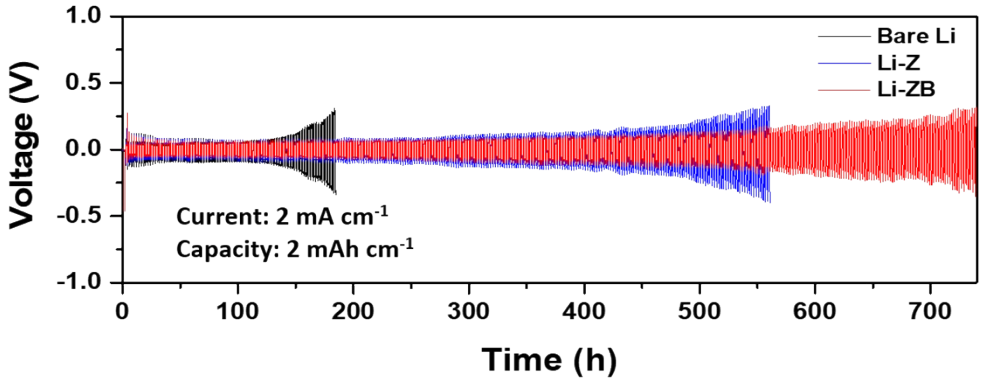

Fig. S12 Cycling stability of symmetric cells using bare Li, Li-Z, and Li-ZB electrodes at a current density of 2 mA cm^{-2} and a deposition capacity of 2 mA h cm^{-2}, respectively.

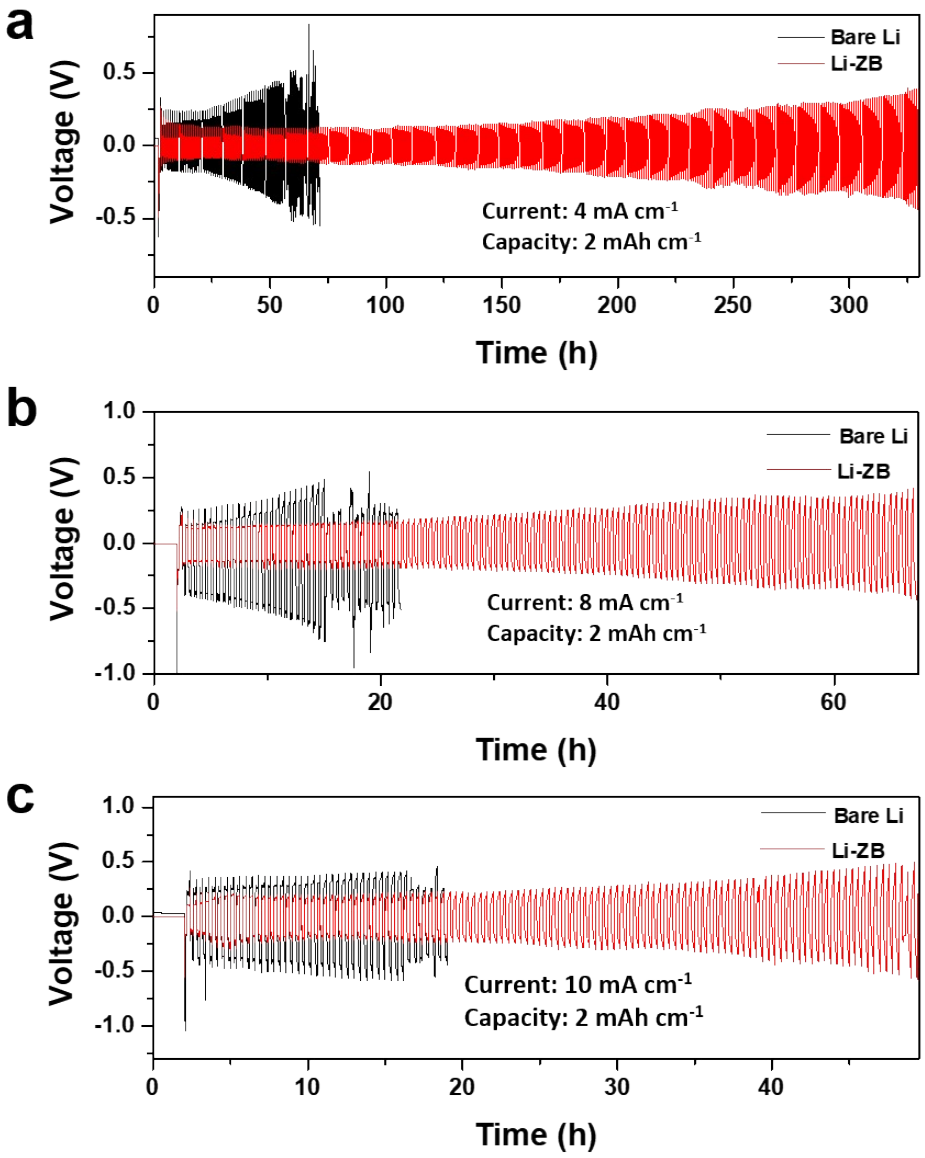

Fig. S13 Cycling stability of Li-ZB anodes at a high rate of (a) 2 C (a current density of 4 mA cm^{-2} and a deposition capacity of 2 mA h cm^{-2}), (b) 4 C (a current density of 8 mA cm^{-2} and a deposition capacity of 2 mA h cm^{-2}), and (c) 5 C (a current density of 10 mA cm^{-2} and a deposition capacity of 2 mA h cm^{-2}).

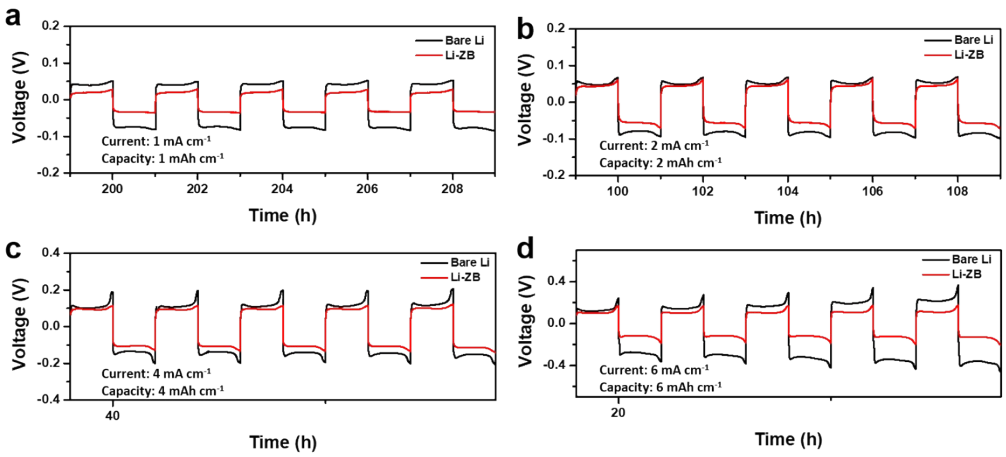

Fig. S14 Voltage profiles of the symmetric cells at various current densities and deposition capacities of (a) 1 mA cm^{-2} and 1 mA h cm^{-2}, (b) 2 mA cm^{-2} and 2 mA h cm^{-2}, (c) 4 mA cm^{-2} and 4 mA h cm^{-2}, (d) 6 mA cm^{-2} and 6 mA h cm^{-2}.

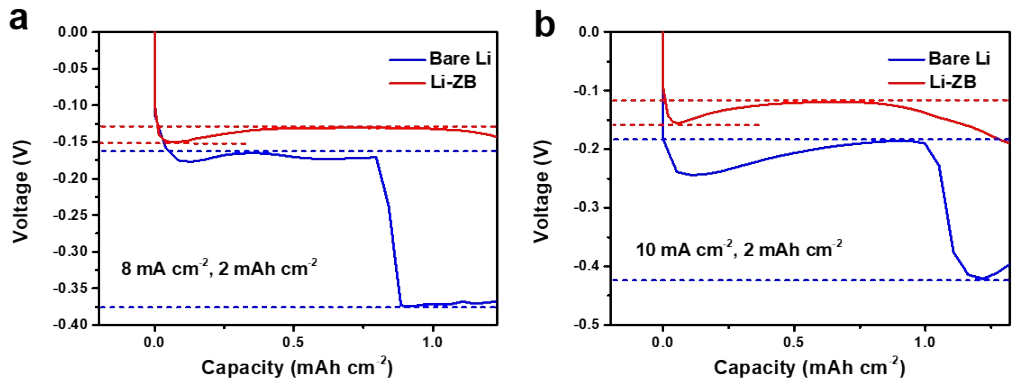

Fig. S15 Voltage-capacity curves of Li-ZB and bare Li electrode during Li plating at current densities and deposition capacities of (a) 8 mA cm^{-2}, 2 mA h cm^{-2} and (b) 10 mA cm^{-2}, 2 mA h cm^{-2}.

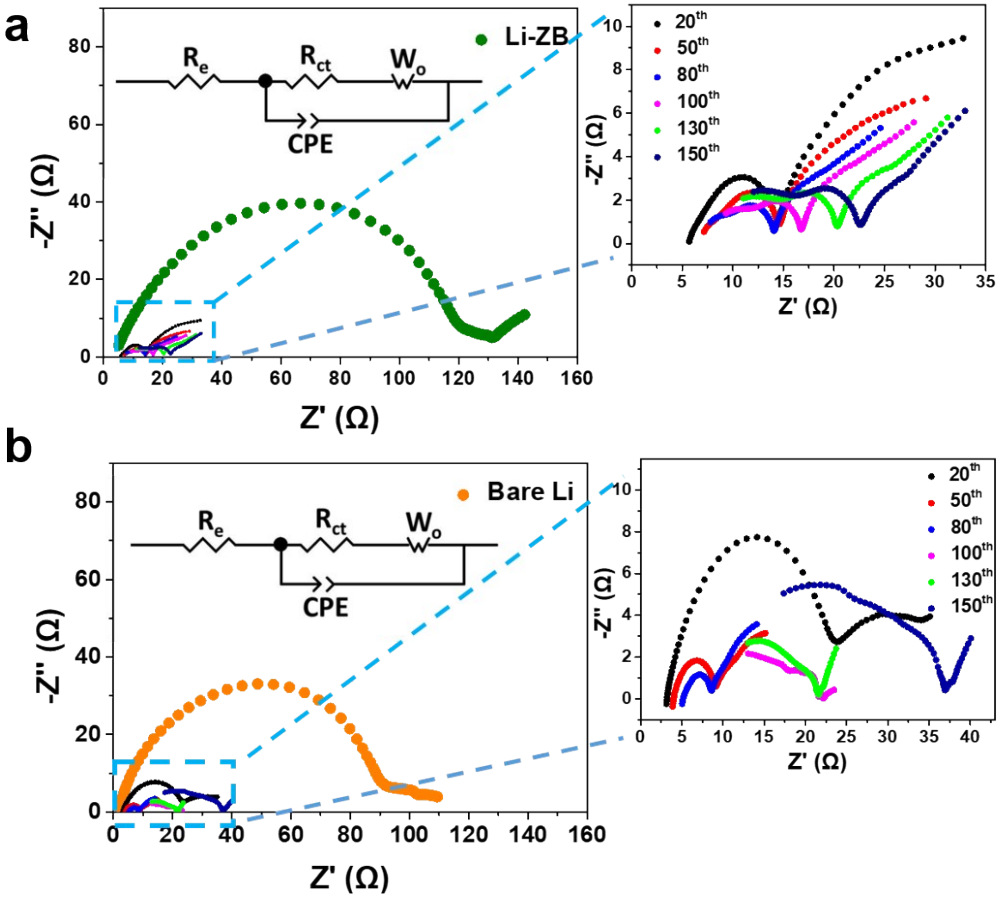

Fig. S16 Nyquist plots of the symmetric cells using (a) Li-ZB and (b) bare Li electrodes at the initial stage and after the 20, 50, 80, 100, 130, and 150 cycles, respectively.

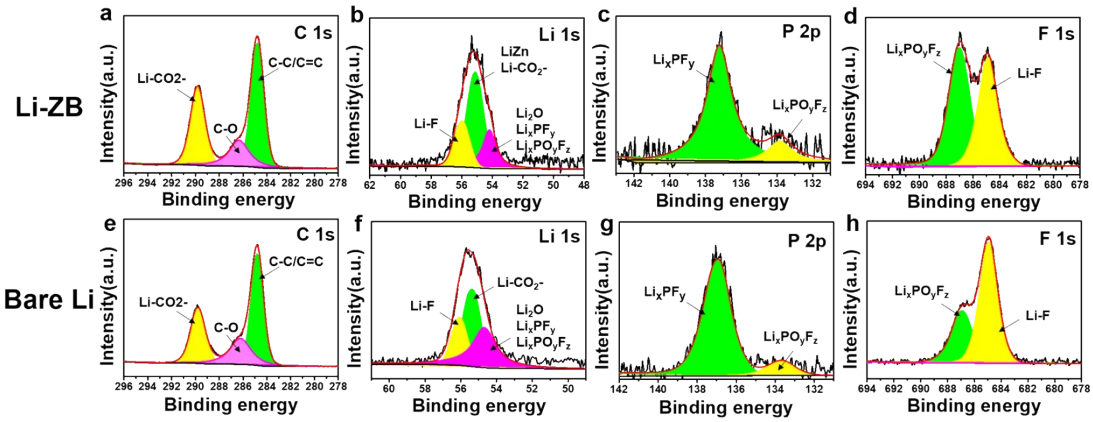

Fig. S17 High-resolution XPS spectra of (a) C 1s, (b) Li 1s, (c) P 2p, (d) F 1s of the Li-ZB electrode, and (e) C 1s, (f) Li 1s, (g) P 2p, (h) F 1s of the bare Li electrode after cycling at a current density of 2 mA cm^{-2} and a deposition capacity of 2 mA h cm^{-2}.

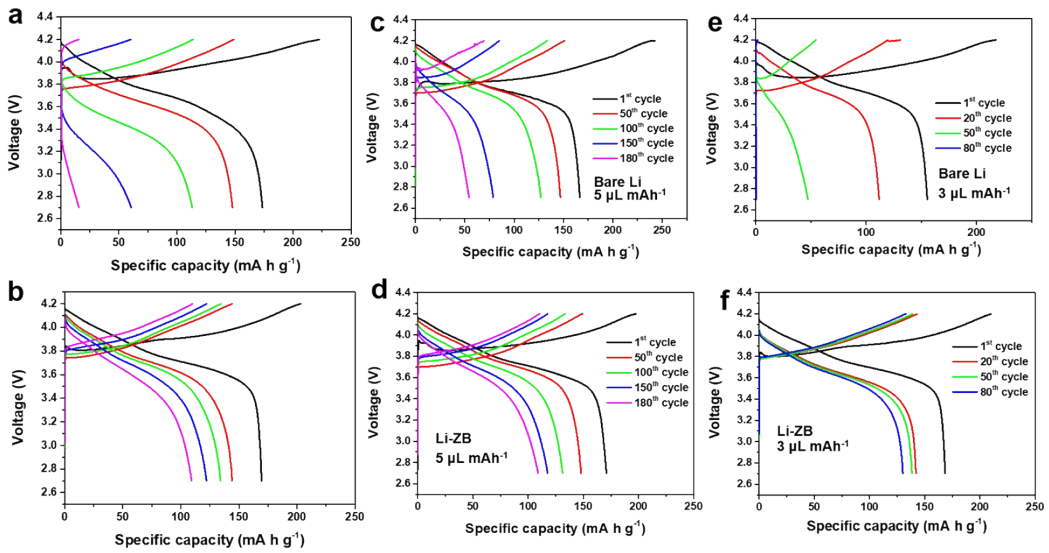

Fig. S18 Charge/discharge profiles of full cells using bare Li as anode under a flooded-electrolyte condition (a) and lean-electrolyte conditions of (c) 5 μL mAh^{-1} and (e) 3 μL mAh^{-1}. Charge/discharge profiles of full cells using Li-ZB as anode under a flooded-electrolyte condition (b) and lean-electrolyte conditions of (d) 5 μL mAh^{-1} and (f) 3 μL mAh^{-1}.

2. Supplementary Table

Table S1 Zeta potential of h-BN in carbonate electrolyte.

Sample ID	Solvent	Temperature (°C)	Zeta Potential (mV)	Mobility (μ/s)/(V/cm)	Conductance (μS)
BN-1	1 M $LiPF_6$ in EC/DEC (1:1 by volume)	25	48.90	3.29	9,577
BN-2		25	50.20	3.41	9,577
BN-3		25	68.50	4.22	9,577

3. Supplementary videos

Video S1 The molten Li was infused into the ZB film to get Li-ZB.

Video S2 Li plating behavior on the bare Li electrode investigated by optical microscopy.

Video S3 Li plating behavior on the Li-ZB electrode investigated by optical microscopy.